

Computational model of the migrating motor complex of the small intestine

E. A. Thomas,¹ H. Sjövall,² and J. C. Bornstein¹

¹Department of Physiology, University of Melbourne, Parkville 3010, Australia;

and ²Department of Internal Medicine, Sahlgrenska University Hospital, S-413 45 Göteborg, Sweden

Submitted 28 August 2003; accepted in final form 13 November 2003

Thomas, E. A., H. Sjövall, and J. C. Bornstein. Computational model of the migrating motor complex of the small intestine. *Am J Physiol Gastrointest Liver Physiol* 286: G564–G572, 2004. First published November 20, 2003; 10.1152/ajpgi.00369.2003.—The migrating motor complex (MMC) is a cyclic motor pattern with several phases enacted over the entire length of the small intestine. This motor pattern is initiated and coordinated by the enteric nervous system and modulated by extrinsic factors. Because *in vitro* preparations of the MMC do not exist, it has not been possible to determine the intrinsic nerve circuits that manage this motor pattern. We have used computer simulation to explore the possibility that the controlling circuit is the network of AH/Dogiel type II (AH) neurons. The basis of the model is that recurrent connections between AH neurons cause local circuits to enter a high-firing-rate state that provides the maximal motor drive observed in *phase III* of the MMC. This also drives adjacent segments of the network causing slow migration. Delayed negative feedback within the circuit, provided by activity-dependent synaptic depression, forces the network to return to rest after passage of *phase III*. The anal direction of propagation is a result of slight anal bias observed in projections of AH neurons. The model relates properties of neurons to properties of the MMC cycle: *phase III* migration speed is governed by neuron excitability, MMC cycle length is governed by the rate of recovery of synaptic efficacy, and *phase III* duration is governed by duration of slow excitatory postsynaptic potentials in AH neurons. In addition, the model makes experimental predictions that can be tested using standard techniques.

neural networks; recurrent excitation; synaptic depression; enteric nervous system; waves in neural tissue; motor pattern generation

THE SMALL INTESTINE SHOWS a remarkable motor pattern, known as the migrating motor complex (MMC), which consists of several phases of motor activity played out over hours of time and meters of space (10, 11, 40). Three phases of the MMC are usually recognized. *Phase I* is characterized by near quiescence. *Phase II* has intermittent, apparently random, stationary contractions that are weaker than the *phase III* contractions, and either occur in stationary clusters at slow-wave frequency or propagate rapidly over short distances like peristaltic contractions. *Phase III* is a slowly moving region of strong contractile activity with contractions occurring at slow-wave frequency. This can start as proximally as the stomach and terminate as distally as the terminal ileum. The propagation speed of *phase III*, in guinea pig, varies from 17.5 cm/min in the duodenum to 4.1 cm/min in the ileum (13). The duration is ~4 min and is roughly constant along the length of the intestine. In humans, cycle length varies markedly both within and between individuals (median value, 100 min). The duration of human *phase III* is consistently shorter, it propagates faster in the proximal intestine, and only ~10% reach the terminal

ileum with many complexes dying out in the distal ileum (22). Individual contractions within *phase III* occur at slow-wave frequency (34) and are presumably myogenic. Nevertheless, the entire interdigestive cycle is initiated and coordinated by the enteric nervous system (ENS) with the extrinsic innervation having a strong modulatory effect (18, 32, 33, 35). The neural circuits coordinating this motor pattern are unknown, and most of the previous literature has used purely phenomenological descriptions without attempting to define the underlying neurophysiological mechanisms.

Propagation and initiation of *phase III* depends on the ENS so this network of neurons must sustain firing in excitatory motor neurons in broad bands that migrate slowly along the intestine. This firing pattern depends on the neural circuitry within the ENS; that is, the projections and connections between different functional classes of enteric neurons. The guinea pig ileum is the only species and region for which a full accounting of enteric neurons has been made (see Ref. 4 for a review). In guinea pig ileum, functional classes of neurons are interneurons, motor neurons, and AH/Dogiel type II neurons. Interneurons project up to 10 mm orally or 5–70 mm anally with little circumferential spread and appear to form feed forward networks. Both excitatory and inhibitory motor neurons project short distances circumferentially and longitudinally to the smooth muscle. AH/Dogiel type II neurons have recently been identified as intrinsic primary afferent neurons (IPANs) (1, 24) and have several processes that typically project 5–10 mm in both circumferential directions and 0.5–1 mm in longitudinal directions (5). These neurons form synapses with nearby AH/Dogiel type II and transmission through these synapses is by slow excitatory postsynaptic potentials (EPSPs) (25). Therefore, they form local circuits with recurrent excitation (“driver circuits”) and may also act as interneurons (46).

Although interneurons have projections compatible with a role in migration of *phase III* activity, a simple argument (see RESULTS), based on axonal projection length, propagation speed, and time between initiation of a postsynaptic event and subsequent action potential firing, shows that myenteric interneurons will propagate signals too rapidly to reproduce the observed slow speed of *phase III* propagation. The same argument applied to AH/Dogiel type II neurons suggests they are ideally placed to propagate a signal at the speed of *phase III* migration. We therefore propose that activity propagating through the network of AH/Dogiel type II neurons forms the basis of slow *phase III* migration. Transmission between neurons is excitatory, which means that positive feedback within the local recurrent connections will drive the network into a

Address for reprint requests and other correspondence: E. A. Thomas, ¹Dept. of Physiology, Univ. of Melbourne, Parkville 3010, Australia (E-mail: evan@evan-thomas.net).

The costs of publication of this article were defrayed in part by the payment of page charges. The article must therefore be hereby marked “advertisement” in accordance with 18 U.S.C. Section 1734 solely to indicate this fact.

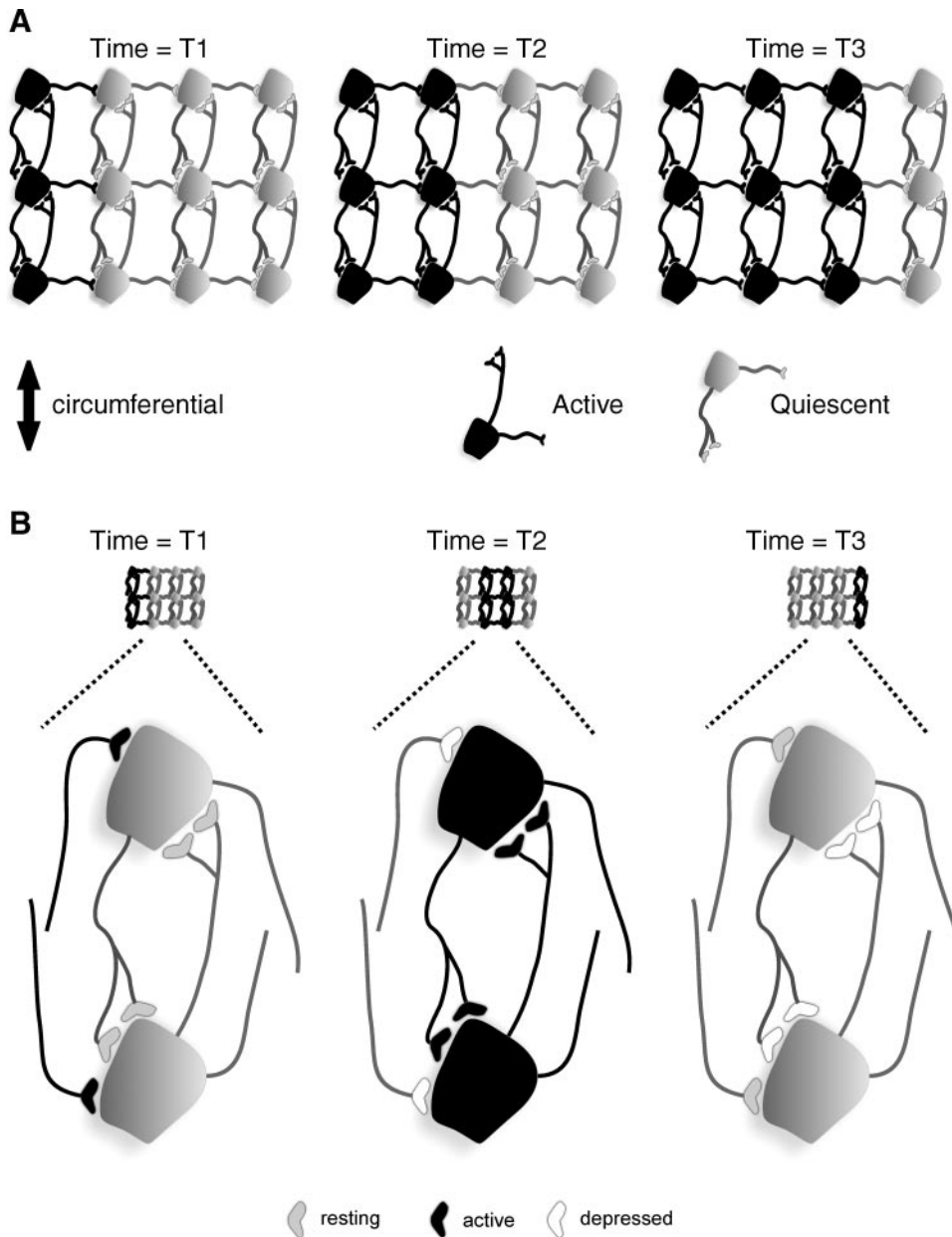


Fig. 1. The model of wave propagation through the network of AH/Dogiel type II neurons. These illustrations represent the pattern of connections between AH/Dogiel type II neurons. Projections are predominantly circumferential but with a longitudinal bias. Only one direction of longitudinal bias is illustrated. *A*: local recurrent connections and strong, slow excitations that drive neurons into a high-firing-rate state, are in black. When neurons are in this state, they are able to excite their neighbors and so activity can propagate longitudinally. Unless another mechanism comes into play, the network will remain in a high-firing-rate state. *B*: illustration of the model analyzed by using numerical simulations. At *time = T1*, active neurons in the leftmost segment of the illustrated network drive neurons in an adjacent segment. At *time = T2*, activity in neurons in the central segments cause these segments to enter a high-firing-rate state and so drive neighboring neurons. Synapses from neurons in the leftmost segment become depressed, terminating drive into this segment. At *time = T3*, synapses in the central segments have become depressed allowing this part of the network to return to rest.

high-firing-rate state. When a section of network is in this state, it can drive adjacent sections into the same state, thus generating propagation (see Fig. 1*A*). High firing will cause depression of synaptic efficacy, reduction of positive feedback, and a return to the quiescent state (see Fig. 1*B*). Anal projections of these neurons are slightly longer than oral projections (5), so this will confer an oral-anal bias in signal propagation.

The aim of the study was to use a computational model to determine the conditions required for the existence of *phase III*-like activity, i.e., slowly migrating, full facilitation of circular muscle contractility in the network of AH/Dogiel type II neurons and to determine how the properties of neurons affect this particular aspect of network behavior. We used numerical simulation of neural networks with anatomically realistic numbers of neurons, realistic patterns of connections, and plausible neuronal and synaptic dynamics (43, 44) with a simple model of activity-dependent depression included in the model of

synaptic transmission. The overall model produces slowly moving waves (segments of full facilitation) of neural activity that have several features in common with initiation, propagation, and timing of *phase III*. It should be stressed that the model does not address the behavior of individual smooth muscle contractions, because slow-wave activity is not part of the present model. Consequently, our use of the word "wave" refers exclusively to neural network activity. By varying parameters in the model, we examined how synaptic and neuronal dynamics and patterns of connections between neurons affected resulting motor patterns. The model is consistent with several observations of interdigestive motility and has made several experimentally testable predictions.

MATERIALS AND METHODS

Methods were previously described in detail (3, 42, 43) and in particular (44). Numbers are expressed as means \pm SD and are drawn

from a normal distribution. Briefly, networks of AH/Dogiel type II neurons were constructed by using realistic anatomical and neurophysiological parameters. Each AH/Dogiel type II neuron made either 4.9 ± 4.0 or 8.3 ± 7.4 connections with other AH/Dogiel type II neurons in a region measuring 5.0 ± 2.3 mm in the circumferential direction and 0.7 ± 0.8 mm in the longitudinal direction with the center of the region located 0.05 ± 0.8 mm anal to the cell body that recreates the observed anal projection bias. These connection numbers encompass those seen in the myenteric plexus of the guinea pig ileum (5). Networks with 4.9 ± 4.0 connections are referred to as low connectivity networks and those with 8.3 ± 7.4 connections are high-connectivity networks. Simulated networks were 25 mm in the oral/anal direction and 5 mm in the circumferential direction and contained $\sim 5,000$ neurons. Network activity is reported as action potential rate per 1-mm circumferential strip and per 100-ms time bin.

The neuron model is based on a leaky-integrate-and-fire model (3, 12, 44) so action potentials are generated when the membrane potential crosses a defined threshold. AH/Dogiel type II neurons transmit to each other by slow EPSPs (25) that have a time course from tens to hundreds of seconds (2, 28) and a nonlinear voltage response. Slow EPSPs are modeled by a set of equations that reproduce this nonlinear response (2). Parameters of the equations are chosen to reproduce EPSPs with time courses within physiological ranges. Duration of slow EPSPs was varied by factors of $\tau_{\text{EPSP}} \in \{1, 2, 3\}$ relative to the values previously used (43, 44), giving durations of 12, 24, and 38 s, respectively, in response to 10 synaptic events in 1 s. Increasing the synaptic input, while holding other parameters constant, increases the rate of rise of the slow EPSP, increases the membrane potential for submaximal events, and increases the duration of a slow EPSP but does not alter the maximum depolarization that can be achieved. Synaptic input was varied by changing the number of connections between neurons, as described above.

In this study, the synaptic strength, s , was subject to activity-dependent synaptic depression according to the following model

$$\tau_s \frac{ds}{dt} = \Delta \sum_i \delta(t - t_i) s + (s_0 - s) \quad (1)$$

where s_0 is the resting synaptic strength, t_i is the presynaptic spike times, τ_s is the rate of recovery, and $\delta(t)$ is the Dirac delta function that describes an idealized pulse. The term $\Delta \delta(t - t_i) s$ means that at spike time t_i the strength is instantaneously changed to Δs . For example, if $\Delta = 0.9$, the synaptic strength is reduced by 10% at each spike. Between spikes, the synaptic strength recovers to s_0 exponentially with time constant τ_s . For long duration spike trains, the synaptic strength will reach an equilibrium value that depends on Δ and τ_s . Because there is no information available regarding the magnitude of Δ and τ_s , these parameters were varied systematically as part of the study. This model is deliberately simple to keep the number of parameters to a minimum, but at the same time reproduces qualitative features of activity-dependent synaptic depression.

These neurons also display a prominent afterhyperpolarizing potential (AHP) after the action potential (16) that is in turn suppressed by the slow EPSP (14). The AHP and its suppression by the slow EPSP was included in most experiments by using a previously described model (43, 44).

Input to AH/Dogiel type II neurons is by large, slow EPSPs coming from other AH/Dogiel type II neurons and by activation of axon terminals in the mucosa (1) or by the activation of mechanosensitive mechanisms in neurites within the myenteric plexus (24). Activation of terminals is detected in the cell body as antidromic action potentials that appear as proximal process potentials (PPPs) and generate somatic action potentials if the membrane is sufficiently depolarized. Responses to physiological perturbations of the intestinal wall were used as exogenous inputs to the AH/Dogiel type II neural network. Model PPPs were just large enough to evoke action potentials in resting neurons. Stimuli were applied by playing random trains of

PPPs, with constant average frequency, into neurons in the central 5×5 mm section of the network. The strength of the stimulus is reported as the average PPP frequency per neuron.

Simulations were undertaken in purpose-developed parallel software (41) written in the C and Python programming languages. The differential equations describing neuron dynamics were integrated by using a third order, explicit, adaptive, Runge-Kutta method (37). Typical simulations required several hours to tens of days of processor time on a high performance computer. Because of the long-run time, the number of runs was limited. Software is freely available by contacting the authors.

RESULTS

Preliminary Analysis

Network propagation speed. Speed of propagation of a wave through a neural network, V , is given approximately by

$$\frac{1}{V} = \frac{1}{v_a} + \frac{\tau_\theta}{L} \quad (2)$$

where v_a is the axonal propagation speed, τ_θ is average time for the synaptic input to drive the membrane potential to threshold (regardless of the type of EPSP), and L is the average projection length. There are several subclasses of descending interneurons in the guinea pig ileum with projections ranging from 5–70 mm (7). Using the shortest projection length of $L = 5$ mm, $v_a = 200$ mm/s (39), and $\tau_\theta = 1,000$ ms (45), then $V = 5$ mm/s. This is fast compared with the observed propagation speed of 0.8 mm/s in guinea pig ileum (13). On the other hand, the average oral-anal projection distance of AH/Dogiel type II neurons is ~ 0.4 mm on average (5), and with $\tau_\theta = 1,000$ ms (28) this gives $V = 0.4$ mm/s. Thus propagation within the AH/Dogiel type II neuron network is consistent with current knowledge.

Network stability and propagation. Because of excitatory transmission between AH/Dogiel type II neurons and their recurrent connections, these networks have substantial positive feedback (43, 44). This is so strong that any activity in the network, for example the result of a small stimulus, will drive firing until all neurons are firing at their maximum rate. Furthermore, the network will remain in this high-firing-rate state after the stimulus is removed, and so it is not biologically useful. In our previous studies (43, 44), we showed that negative feedback in the form of AHPs or inhibitory postsynaptic potential (IPSPs) can remove the high-firing-rate state and allow the network to return to rest in the absence of input. However, networks with AHP or IPSP negative feedback cannot support stable signal propagation in which stable means that the signal can propagate with constant amplitude over indefinite distances. Consider activity in a small section of a network of Dogiel/type II neurons. If the signal is to propagate over long distances, then the activity in one section must drive the activity in the adjacent section to the same level. Because of the reciprocal circumferential connections, input into the driving section is greater than input into the adjacent section. If there is also negative feedback controlling firing within the circuit, then locally the network cannot drive itself to a firing rate greater than the input firing rate. Thus the firing rate will be less in each subsequent section and the signal will decay with distance. This conclusion was supported by extensive numerical simulations of networks with AHPs or IPSPs by using previously described models (44).

Therefore, for the network to support propagation of a *phase III* episode, negative feedback must be delayed so that the network can temporarily enter a high-firing-rate state and then return to rest. In the following, delayed feedback is provided by activity-dependent synaptic depression described by Eq. 1 and this model is illustrated in Fig. 1B.

Network Simulations

Numerical simulations were performed on networks 25 mm in the longitudinal direction and 5 mm in the circumferential direction and where stimuli were applied in the central 5 mm. Neurons in these networks had parameters similar to those previously reported (43, 44) except that synapses displayed activity-dependent synaptic depression. In most experiments, and unless otherwise noted, an AHP was present in neurons, and this was suppressed to 1/1,000th of its resting value by synaptic excitation (residual AHP). This degree of suppression means that these networks are bistable in the absence of synaptic depression and so are able to enter the high-firing-rate state, a necessary condition for activity to propagate into adjacent areas of the network. In some networks, the AHP was completely absent, even in neurons at rest. We characterized the properties of all networks in terms of the synaptic depression parameters: Δ (that determines the relative change in synaptic efficacy after an action potential), τ_s (half-life of recovery of synaptic efficacy), τ_{EPSP} (relative slow EPSP duration), presence or absence of a residual AHP, and number of connections between neurons and stimulus.

Network behaviors could be placed into three broad categories. In the first, the network lacked excitability and activity did not propagate out of the stimulus region. In the second, activity

propagated out of the stimulus region, and traveled to both oral and anal ends of the simulated network. However, these networks were highly excitable and continued to fire at a high rate indefinitely; once in this state, the network cannot change its firing rate up or down and so cannot perform any useful function. The third category of behavior is illustrated in Fig. 2. In this case, activity also propagates out of the stimulus region but the neurons outside the stimulus region return to the quiescent state after a period of firing. In other words, these networks support localized temporal and spatial regions of a “propagating organized imbalance” or waves (36).

The relationship among the parameters τ_{EPSP} , τ_s , and Δ , and the category of behavior is plotted in Fig. 3. For example, when $\tau_{EPSP} = 1$, all networks with τ_s in the range of 20 to 40 s and Δ in the range of 0.9 to 0.95 showed the first type of behavior; no activity propagated out of the stimulus region. When $\tau_{EPSP} = 2$, waves were possible for most values of τ_s and Δ tested. On the other hand, when $\tau_{EPSP} = 3$, most networks were bistable (44) and showed only the second type of behavior. The difference between bistable networks and those that supported waves was not distinct. Some networks, with parameters that made them highly excitable, showed behavior that was intermediate between the two. In these networks, the few millimeters either side of the stimulus did not return to the quiescent state after passage of the first wave, whereas further from the stimulus region, the network displayed isolated waves.

Properties of Waves

Data in this section were generated in networks in which the stimulus was constant in the central 5-mm section of the

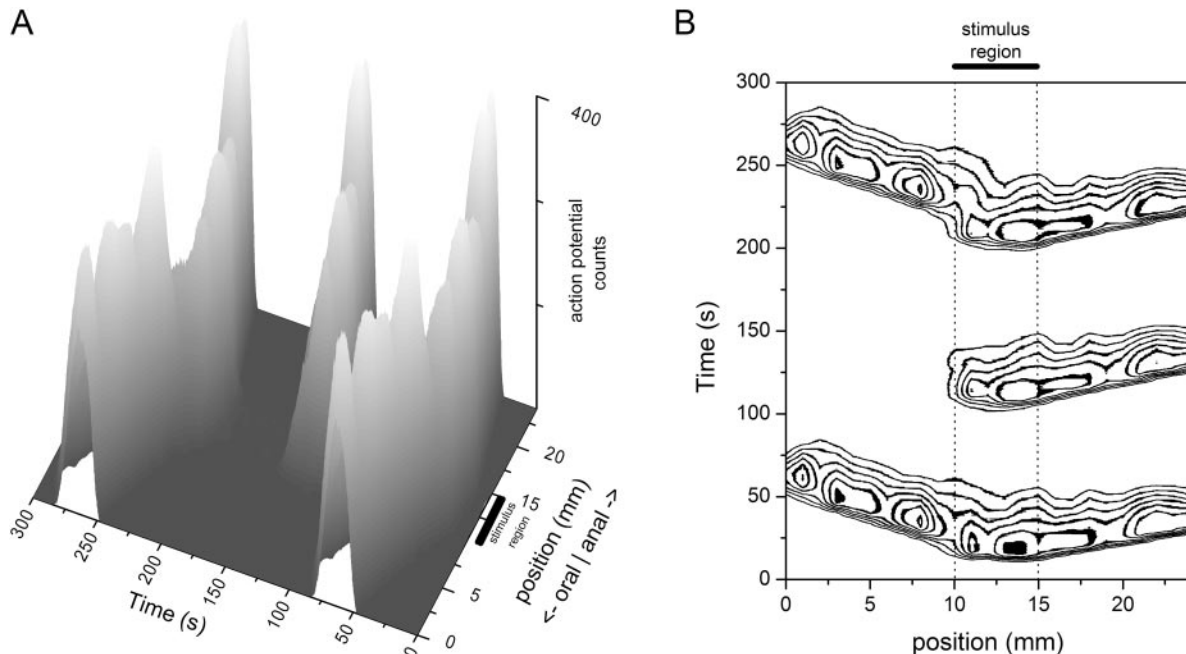


Fig. 2. Waves of activity in a simulated AH/Dogiel type II neural network. Constant stimulus is applied in the 10–15 mm section of the network as indicated by bars. In this network $\Delta = 0.95$, $\tau_s = 30$ s, and $\tau_{EPSP} = 2$. A: this graph plots action potential count per 100-ms time bin and 1-mm spatial bin in the longitudinal direction against time for a network 25-mm long in the longitudinal direction. A constant stimulus of 0.2 Hz has been applied to the central 5 mm, which produces a small response compared with the waves and hence is not clearly visible. Waves of activity propagate out of the stimulus region in both the oral and the anal direction. B: same data, viewed from above, as contours of action potential firing.

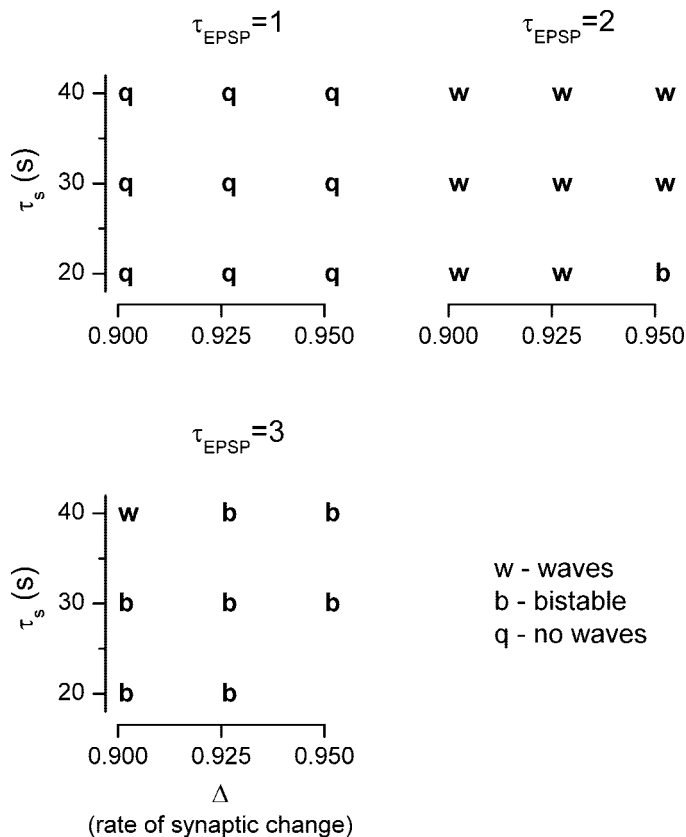


Fig. 3. Outcomes in parameter space. These graphs indicate the classification of networks across a region (τ_{EPSP} , Δ , τ_s) of the parameter space. Networks are classified as **q** when no activity propagated out of the stimulus region, **w** if waves (as defined in the text) were present, and **b** if regions of the networks failed to return to the quiescent state after an activity front propagated through an initially quiescent region.

network and $\tau_{EPSP} = 2$, which meant that slow EPSPs lasted 24 s in response to 10 synaptic events in 1 s.

In networks that supported waves, their peak amplitude at each location in the network showed little dependence on any of the parameters that were varied in this study, although in some cases, the first wave was slightly larger than subsequent waves. As can be seen in Fig. 2, there was some variation in the amplitude of network activity along the longitudinal axis. This was due to variation in the number of convergent synapses along the simulated network, rather than, for instance, the variation in neuron density. In regions in which the network displayed highest activity, neurons were firing near 20 Hz, which is the highest firing rate of the simulated neurons.

Propagation speed of the first wave to emerge from the stimulus region varied from 0.18 to 0.72 mm/s in the oral direction and 0.37 to 1.1 mm/s in the anal direction. Anterograde waves were always faster than retrograde waves. Propagation speed increased when the network was made more excitable by increasing Δ toward 1, decreasing the relative change in synaptic efficacy per action potential, or increasing the number of connections. On the other hand, when other parameters were held constant, increasing τ_s (the time constant of synaptic recovery) decreased propagation speed only slightly. When multiple waves emerged from a region receiving a constant stimulus, the first wave was usually faster than

subsequent waves. For example, for the case of $\Delta = 0.95$ and $\tau_s = 50$ s, the speed of the first wave propagated at 0.72 mm/s and the speed of subsequent waves was 0.55 mm/s. This is because synapses had not completely recovered their efficacy after the passage of the first wave, effectively lowering the excitability of the network. Propagation speeds for the first anally directed wave for various values of τ_s , Δ , and network connectivity are shown in Fig. 4.

In many cases, waves continued to emerge periodically from the stimulus region, propagating either in both directions or only in the anal direction, while the stimulus was maintained. Periods ranged from 70–230 s for anally directed waves and 110–230 s for orally directed waves. In some cases, waves propagating in both directions emerged simultaneously; otherwise, orally directed waves had longer periods. Parameters with the strongest influence on periodicity were the synaptic recovery time constant τ_s and the stimulus strength. For example, when $\Delta = 0.95$ and $\tau_s = 40$ s, the period of anterograde waves was 230 s, when the stimulus was 0.1 Hz, and the period was 80 s, when the stimulus was 0.5 Hz or 2 Hz. Increasing τ_s increased the period between waves for the same stimulus; however, at some point, only a single wave would emerge from the stimulus region. For example, this was the case when $\Delta = 0.95$ and $\tau_s = 60$ s, although the simulation lasted 3,000 s.

The duration of anally directed waves was always greater than the duration of orally directed waves and was independent of stimulus strength. Increasing excitability of the network by increasing Δ , decreasing τ_s , increasing the number of connections, or removing the AHP, increased wave duration. Some of these data are summarized in Fig. 5.

Number of Connections Between Neurons

Networks with different numbers of connections between neurons were generated so that results can be generalized to other regions and species. In one network, there were 8.3 ± 7.4 connections per neuron and in the other, 4.9 ± 4.0 connections per neuron. A number of runs were carried out with networks that differed only in the number of connections. Networks with

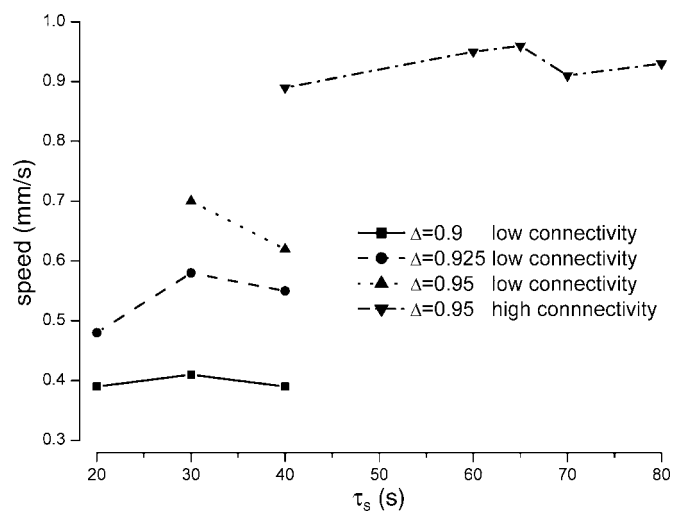


Fig. 4. Wave speed is plotted as a function of the synaptic recovery time constant (τ_s) for different values of Δ and number of connections between neurons. Low connectivity corresponds to 4.9 ± 4.0 (mean \pm SD) connections between neurons, and high connectivity corresponds to 8.3 ± 7.4 connections.

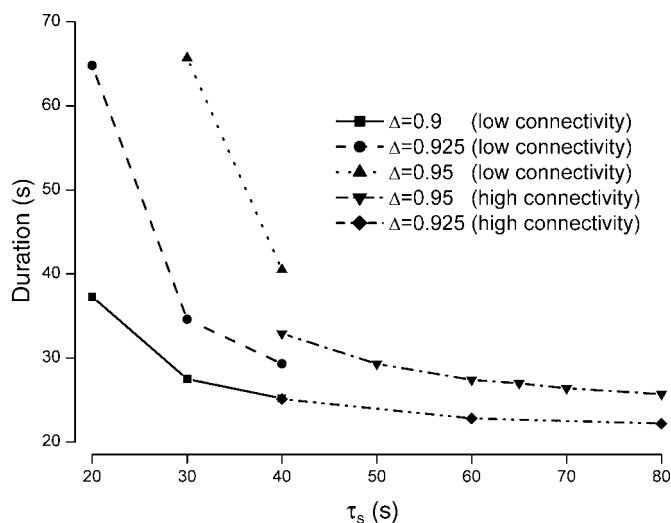


Fig. 5. Wave duration is plotted as a function of the synaptic recovery time constant (τ_s) for different values of Δ and number of connections between neurons. Low connectivity corresponds to 4.9 ± 4.0 (mean \pm SD) connections between neurons, and high connectivity corresponds to 8.3 ± 7.4 connections.

more connections had faster propagation speeds. When networks showed periodically, emerging waves increasing the number of connections decreased the period, and when only one wave emerged during a simulation, increasing the number of connections restored periodically emerging waves.

Effect of AHP

At rest, AH/Dogiel type II neurons display a prominent AHP after the action potential (16), and although the underlying current is suppressed during slow EPSPs (14), it may affect firing during the near-quiescent phases of wave activity. Completely removing the AHP from neurons, even at rest, increased network excitability, but had only a small effect on wave properties. In some cases, periodically emerging waves could be recovered from networks with large values of τ_s . For example, when $\Delta = 0.95$, $\tau_s = 80$ s, and neurons had AHPs, only a single wave emerged from the stimulus region in 300 s of simulation. Removing the AHP caused another anterograde and a retrograde wave to emerge after 93 and 110 s, respectively. When τ_s was increased to 120 s, a second anterograde wave emerged after 445 s.

Effect of Slow EPSP Duration on Waves

AH/Dogiel type II neurons display slow EPSPs with durations that range from seconds (28) to minutes (6) to hours (9). Increasing the slow EPSP duration while keeping other parameters constant made the network bistable in most cases. However, when this did not occur, wave duration was increased considerably. For example, when $\Delta = 0.95$ and $\tau_s = 40$ s, increasing τ_{EPSP} from 2 to 3 increased wave duration from 25 to 74 s and when $\Delta = 0.925$ and $\tau_s = 60$ s, increasing τ_{EPSP} from 2 to 3 increased wave duration from 23 to 61 s. Waves with $\tau_{EPSP} = 3$ were robust in other parts of τ_s and Δ parameter space, and these had durations greater than waves with the lower values of the slow EPSP duration.

Different Stimulus Protocols

In networks in which multiple waves emerged from the stimulus region, initial increases in τ_s increased the period between waves. However, once a certain point was reached, further increases in τ_s elicited only a single wave from the stimulus region, even when the simulation was many times longer than τ_s .

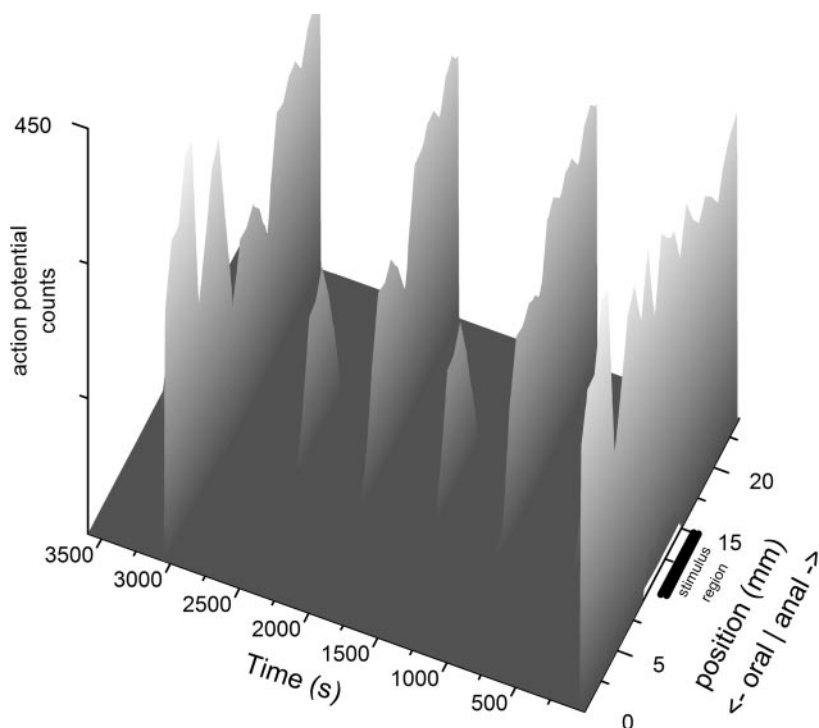
The stimulus used for the previous data was constant in time, which is not physiologically realistic, so we performed four simulations in which the stimulus consisted of regular brief pulses to mimic sensory input from random or spontaneous events. An example from a run using this protocol is illustrated in Fig. 6 in which 2 Hz average PPP input is applied to every neuron in the central 5 mm of the simulated network for 5 s every 500 s, and other parameters were $\tau_s = 1,000$ s, $\Delta = 0.95$, and $\tau_{EPSP} = 2$. Anterograde waves emerge on every second stimulus giving a period of 1,000 s, and a second retrograde wave also emerged after 3,000 s. When $\tau_s = 2,000$ s with other parameters the same, only a single wave emerged from the stimulus region. When $\tau_s = 80$ s and 10-s pulses were used, a retrograde and anterograde wave emerged from the stimulus region at each stimulus.

DISCUSSION

The key finding of the present study is that the network of AH/Dogiel type II neurons may be the circuit that initiates and coordinates the MMC phenomenon. This is the simplest circuit that might account for this motor pattern and we have identified three groups of parameters that decisively affect behavior of the system and may be subject to physiological modulation: parameters that affect network excitability, rate of synaptic recovery, and duration of slow EPSP. It is important that parameters must be within an interrelated range of values for two reasons: 1) to provide a high-firing-rate state able to generate both the maximal motor drive characteristic of *phase III*, enabling propagation; and 2) to enable the network to return to the quiescent state characteristic of *phase I*. When parameters are within this range, network excitability determines *phase III* migration speed and has a small effect on the interval between *phase III*. Synaptic recovery half life has a major effect on the interval between *phase III* episodes. When the stimulus is constant, the interval between *phase III* episodes is limited to a few hundred seconds (Figs. 2 and 5), however, when the stimulus is not constant, the interval between *phase III* episodes can be arbitrarily controlled by the synaptic recovery time (Fig. 6). Duration of each wave is controlled by duration of slow EPSP. It is likely that increased motor activity of *phase II* occurs as synapses recover, and the network becomes more excitable and is in a position to drive other motor patterns in response to sensory input, although this was not explicitly simulated in our model.

Waves of neural firing have a distinct anal bias in that anally directed waves are always faster and usually more common than orally directed waves. The only asymmetry in the network is the slight anal bias of projections along the oral-anal axis, so this must be the cause of the consistent anal propagation of the MMC. Waves that are all or nothing mean that their properties are independent of the stimulus once the stimulus is large enough to generate a wave.

Fig. 6. Waves generated in response to an intermittent stimulus. Data are similar to those in Fig. 2, except that the stimulus is 2 Hz applied for 5 s every 500 s in the 10–15 mm section of the network as indicated. Network parameters are $\Delta = 0.95$, $\tau_s = 1,000$ s, and $\tau_{EPSP} = 2$.



Most building blocks of the model closely match known physiology; however, an important component of the model is “delayed negative feedback,” which is required to bring network firing back to rest after the passage of a wave. The most likely candidate for this is activity-dependent synaptic depression. Little is known about synaptic plasticity in the ENS, but there are some mechanisms that might lead to synaptic plasticity of the form used in this model. Time scales for synaptic recovery that are relevant to the model we are proposing are around 100–200 min corresponding to an inter-*phase III* interval of 140 min in guinea pig (13). Both neurokinin-1 and -3 receptors are present on AH/Dogiel type II neurons and have been shown to internalize in the presence of transmitter candidates (20, 27, 38), and neurokinin-1 receptors return to the surface on a timescale of 120–180 min (20). Other potential sources of plasticity include presynaptic inhibition at muscarinic receptors (29, 30) mediated by acetylcholine that is released by AH/Dogiel type II neurons (21). More speculatively, transmitter may deplete in synapses during the long periods of high firing (47), and, because tachykinins require transport from the soma, this may cause a slow recovery period of the type required for the model.

Predictions of the model are consistent with several observations. First, initiation of *phase III* is highly variable both in location and time, even within individuals (22). In the proposed model, there is no specific “clock” that initiates the next *phase III*; rather it is triggered by a spontaneous event in a region in which synapses have recovered sufficiently to allow propagation. The random nature of the trigger provides the variability in both time and location. Because proximal regions of the network recover earlier, this is the region in which the next event is most likely to initiate. This predicts that distally initiated events are correlated with a longer interval since the previous event. The anal bias of AH/Dogiel type II neuron

projections naturally explains the propensity of *phase III*s to propagate anally; however, numerical simulations show oral waves are also possible. Normally these will not be seen, because anal waves are much more likely, but if the network is hyperexcitable, a *phase III*-like event can propagate orally, and this is seen in some pathological conditions (19).

Transit of *phase III* is blocked by close interarterial perfusion of atropine (32) that blocks excitatory transmission to the muscle (15). This might be interpreted to mean that mechanical feedback from the muscle is required for *phase III* migration, because a purely neurogenic wave should propagate through the region of atropine perfusion. An alternative explanation for the blockade of *phase III* transit is that atropine may interfere with synaptic transmission (31) or synaptic depression (30) by blocking pre- or postsynaptic muscarinic receptors and move the network into a parameter regimen in which propagation is not possible.

The fundamental prediction of the model is that networks of AH/Dogiel type II neurons support signal propagation over large distances. This should be testable by using standard preparations and electrophysiological techniques (e.g., Ref. 16). We are aware of only a single report (17) of responses seen in AH/Dogiel type II neurons to longitudinally distant stimuli, and latencies were not reported. In typical electrophysiological studies, the mucosa is removed for several millimeters from the site of impalement, but it is now recognized that the mucosa has a profound effect on enteric neuron excitability (23). Furthermore, the speed of propagation anticipated for these networks in the ileum means that the latency of the response would be tens of seconds, rather than the hundreds of milliseconds seen for S neurons, and long latency events may not have been correlated with the stimulus. Thus this prediction remains to be adequately tested.

Another prediction of the model is based on the observation that there is a decreasing gradient of *phase III* propagation speed along the intestine (13), and this suggests there is a gradient in the properties of the AH/Dogiel type II neurons along the intestine. In the model, propagation is always faster in the anal direction because of the longer anal projections of the AH/Dogiel type II neurons. Thus the model predicts that a systematic reduction in the bias of projections will lead to a systematic reduction in the propagation speed. This is straightforward to test using standard immunohistochemical techniques (5). Alternatively, excitability of AH/Dogiel type II neurons may decrease distally through a number of mechanisms. Examples of such mechanisms are that slow EPSPs may have slower rise times, or shorter durations or membrane currents may lead to reduced firing. A proportion of AH/Dogiel type II neurons in the duodenum lack an AHP (8) and so these networks may be more excitable than their counterparts in the ileum. A better understanding of the mechanisms that lead to slower propagation and eventual extinction of *phase III* in the ileum are potentially important, because this function will markedly affect both the fluid load on the colon and the time available for such functions as bile acid reuptake. Our model provides a theoretical framework to experimentally approach this potentially important function.

In conclusion, we propose that the intrinsic circuits coordinating the MMC are those circuits formed by the recurrent connections of AH/Dogiel type II neurons. These neurons are now known to be IPANs (1, 24); however, it has been speculated for some time that they have a role in coordinating intestinal reflexes (46). We describe a few important parameters that will be decisive for the behavior of this pattern-generating system and propose how these predictions can be tested experimentally. There is growing evidence that neurons have roles in more than one motor pattern (26), thus it is likely that these circuits play a major role in many intestinal motor patterns and have a pivotal role in switching between motor patterns.

ACKNOWLEDGMENTS

We are grateful to Paul Bertrand, Jordan Chambers, Phil Davies, and Rebecca Monro for valuable comments on the manuscript.

GRANTS

This work was supported by Grant DP0210004 from the Australian Research Council, Grant 8288 from the Swedish Medical Research Council, and a Victorian Partnership for Advanced Computing Expertise grant. Computer facilities were provided by the Victorian Partnership for Advanced Computing.

REFERENCES

- Bertrand PP, Kunze WA, Bornstein JC, Furness JB, and Smith ML. Analysis of the responses of myenteric neurons in the small intestine to chemical stimulation of the mucosa. *Am J Physiol Gastrointest Liver Physiol* 273: G422–G435, 1997.
- Bertrand PP, Thomas EA, Kunze WAA, and Bornstein JC. A simple mathematical model of second-messenger mediated slow excitatory postsynaptic potentials. *J Comput Neurosci* 8: 127–142, 2000.
- Bornstein JC, Furness JB, Kelly HF, Bywater RAR, Neild TO, and Bertrand PP. A computer simulation of the enteric nervous system. *J Auton Nerv Syst* 64: 143–157, 1997.
- Bornstein JC, Furness JB, Kunze WA, and Bertrand PP. Enteric reflexes that influence motility. In: *Innervation of the Gastrointestinal Tract*, edited by Costa M and Brookes SJ, 2002.
- Bornstein JC, Hendriks R, Furness JB, and Trussell DC. Ramifications of the axons of AH-neurons injected with the intracellular marker biocytin in the myenteric plexus of the guinea pig small intestine. *J Comp Neurol* 314: 437–452, 1991.
- Bornstein JC, North RA, Costa M, and Furness JB. Excitatory synaptic potentials due to activation of neurons with short projections in the myenteric plexus. *Neuroscience* 11: 723–731, 1984.
- Brookes S. Retrograde tracing of enteric neuronal pathways. *Neurogastroenterol Motil* 13: 1–18, 2001.
- Clerc N, Furness JB, Bornstein JC, and Kunze WA. Correlation of electrophysiological and morphological characteristics of myenteric neurons of the duodenum in the guinea pig. *Neuroscience* 82: 899–914, 1998.
- Clerc N, Furness JB, Kunze WAA, Thomas EA, and Bertrand PP. Long-term effects of synaptic activation at low frequency on enteric neurons. *Neuroscience* 90: 279–289, 1999.
- Code CF and Marlett JA. The interdigestive myo-electric complex of the stomach and small bowel of dogs. *J Physiol* 246: 289–309, 1975.
- Ehrlein HJ, Schemann M, and Siegle ML. Motor patterns of small intestine determined by closely spaced extraluminal transducers and videofluoroscopy. *Am J Physiol Gastrointest Liver Physiol* 253: G259–G267, 1987.
- Gabbiani F and Koch C. Principles of spike train analysis. In: *Methods in Neuronal Modeling: from Ions to Networks*, edited by Segev CKaI, 1998.
- Galligan JJ, Costa M, and Furness JB. Gastrointestinal myoelectric activity in conscious guinea pigs. *Am J Physiol Gastrointest Liver Physiol* 249: G92–G99, 1985.
- Grafe P, Mayer CJ, and Wood JD. Synaptic modulation of calcium-dependent potassium conductance in myenteric neurones in the guinea pig. *J Physiol* 305: 235–248, 1980.
- Hirst GD, Holman ME, and McKirdy HC. Two descending nerve pathways activated by distension of guinea pig small intestine. *J Physiol* 244: 113–127, 1975.
- Hirst GD, Holman ME, and Spence I. Two types of neurones in the myenteric plexus of the duodenum in the guinea pig. *J Physiol* 236: 303–326, 1974.
- Hodgkiss JP and Lees GM. Slow intracellular potentials in AH-neurons of the myenteric plexus evoked by repetitive activation of synaptic inputs. *Neuroscience* 11: 255–261, 1984.
- Itoh Z, Aizawa I, and Takeuchi S. Neural regulation of interdigestive motor activity in canine jejunum. *Am J Physiol Gastrointest Liver Physiol* 240: G324–G330, 1981.
- Jebbink HJ, vanBerge-Henegouwen GP, Akkermans LM, and Smout AJ. Small intestinal motor abnormalities in patients with functional dyspepsia demonstrated by ambulatory manometry. *Gut* 38: 694–700, 1996.
- Jenkinson KM, Mann PT, Southwell BR, and Furness JB. Independent endocytosis of the NK₁ and NK₃ tachykinin receptors in neurons of the rat myenteric plexus. *Neuroscience* 100: 191–199, 2000.
- Johnson PJ, Bornstein JC, Yuan SY, and Furness JB. Analysis of contributions of acetylcholine and tachykinins to neuro-neuronal transmission in motility reflexes in the guinea pig ileum. *Br J Pharmacol* 118: 973–983, 1996.
- Kellow JE, Borody TJ, Phillips SF, Tucker RL, and Haddad AC. Human interdigestive motility: variations in patterns from esophagus to colon. *Gastroenterology* 91: 386–395, 1986.
- Kunze WA, Bertrand PP, Furness JB, and Bornstein JC. Influence of the mucosa on the excitability of myenteric neurons. *Neuroscience* 76: 619–634, 1997.
- Kunze WA, Bornstein JC, and Furness JB. Identification of sensory nerve cells in a peripheral organ (the intestine) of a mammal. *Neuroscience* 66: 1–4, 1995.
- Kunze WA, Furness JB, and Bornstein JC. Simultaneous intracellular recordings from enteric neurons reveal that myenteric AH neurons transmit via slow excitatory postsynaptic potentials. *Neuroscience* 55: 685–694, 1993.
- Lieske SP, Thoby-Brisson M, Telgkamp P, and Ramirez JM. Reconfiguration of the neural network controlling multiple breathing patterns: eupnea, sighs and gasps. *Nat Neurosci* 3: 600–607, 2000.
- Mann PT, Southwell BR, and Furness JB. Internalization of the neurokinin 1 receptor in rat myenteric neurons. *Neuroscience* 91: 353–362, 1999.
- Morita K and North RA. Significance of slow synaptic potentials for transmission of excitation in guinea pig myenteric plexus. *Neuroscience* 14: 661–672, 1985.

29. **Morita K, North RA, and Tokimasa T.** Muscarinic presynaptic inhibition of synaptic transmission in myenteric plexus of guinea pig ileum. *J Physiol* 333: 141–149, 1982.
30. **North RA, Slack BE, and Surprenant A.** Muscarinic M₁ and M₂ receptors mediate depolarization and presynaptic inhibition in guinea pig enteric nervous system. *J Physiol* 368: 435–452, 1985.
31. **North RA and Tokimasa T.** Muscarinic synaptic potentials in guinea pig myenteric plexus neurones. *J Physiol* 333: 151–156, 1982.
32. **Sarna S, Condon RE, and Cowles V.** Enteric mechanisms of initiation of migrating myoelectric complexes in dogs. *Gastroenterology* 84: 814–822, 1983.
33. **Sarna S, Stoddard C, Belbeck L, and Mewade D.** Intrinsic nervous control of migrating myoelectric complexes. *Am J Physiol Gastrointest Liver Physiol* 241: G16–G23, 1981.
34. **Sarna SK.** Cyclic motor activity; migrating motor complex: 1985. *Gastroenterology* 89: 894–913, 1985.
35. **Sarr MG and Kelly KA.** Myoelectric activity of the autotransplanted canine jejunioileum. *Gastroenterology* 81: 303–310, 1981.
36. **Scales JA and Snieder R.** What is a wave? *Nature* 401: 739–740, 1999.
37. **Shampine LF.** Numerical solution of ordinary differential equations. 1994.
38. **Southwell BR, Seybold VS, Woodman HL, Jenkinson KM, and Furness JB.** Quantitation of neurokinin 1 receptor internalization and recycling in guinea pig myenteric neurons. *Neuroscience* 87: 925–931, 1998.
39. **Stebbing MJ and Bornstein JC.** Electrophysiological mapping of fast excitatory synaptic inputs to morphologically and chemically characterized myenteric neurons of guinea pig small intestine. *Neuroscience* 73: 1017–1028, 1996.
40. **Szurszewski JH.** A migrating electric complex of canine small intestine. *Am J Physiol* 217: 1757–1763, 1969.
41. **Thomas EA.** A parallel algorithm for simulation of large neural networks. *J Neurosci Methods* 98: 123–134, 2000.
42. **Thomas EA, Bertrand PP, and Bornstein JC.** Genesis and role of coordinated firing in a feed forward network—a model study of the enteric nervous system. *Neuroscience* 93: 1525–1537, 1999.
43. **Thomas EA, Bertrand PP, and Bornstein JC.** A computer simulation of recurrent, excitatory networks of sensory neurons of the gut in guinea pig. *Neurosci Lett* 287: 137–140, 2000.
44. **Thomas EA and Bornstein JC.** Inhibitory cotransmission or afterhyperpolarizing potentials can regulate firing in recurrent networks with excitatory metabotropic transmission. *Neuroscience* 120: 333–351, 2003.
45. **Thornton PD and Bornstein JC.** Slow excitatory synaptic potentials evoked by distension in myenteric descending interneurons of guinea pig ileum. *J Physiol* 539: 589–602, 2002.
46. **Wood JD.** Functions of AH/Dogiel II and S/Dogiel I neurons in the enteric microcircuits. In: *Advances in the Innervation of the Gastrointestinal Tract*, edited by G. E. Holle JDW. Amsterdam: Excerpta Medica, 1992, p. 125–145.
47. **Zucker RS and Regehr WG.** Short-term synaptic plasticity. *Annu Rev Physiol* 64: 355–405, 2002.

